

Computation of Selected Optical Transitions of Diatomic Molecules: AlO, C₂, CN, OH, N₂⁺, NO, and TiO

CHRISTIAN G. PARIGGER

*Physics and Astronomy Department, University of Tennessee,
University of Tennessee Space Institute, Center for Laser Applications,
411 B.H. Goethert Parkway, Tullahoma, TN 37388-9700, USA; cparigge@tennessee.edu*

ABSTRACT: This work communicates spectra and associated scripts for computation and spectroscopic fitting of selected transitions of the diatomic molecules AlO, C₂, CN, OH, N₂⁺, NO, and TiO. For ease of use, the scripts for data analysis are designed for inclusion in various software packages or program languages. The accuracy of the data is of the order of less than one picometer, suitable for analysis of laser-induced fluorescence and laser-plasma spectra. Selected results demonstrate the applicability of the program for data analysis in laser-induced optical breakdown spectroscopy primarily at The University of Tennessee Space Institute, Center for Laser Applications. Representative spectra are calculated and referenced to measured data records.

KEYWORDS: Diatomic molecules; Laser-plasma; Data analysis; Laser induced breakdown spectroscopy; Combustion; Spectroscopy, Spectra fitting program; Astrophysics

1. INTRODUCTION

Atomic, molecular, optical (AMO) spectroscopy furnishes fundamental insight by decoding light emanating from targets of interest [1–8]. Analytical studies of elements maybe straightforward, especially for elements that appear in the first three rows of the period table. Balmer series hydrogen lines or sodium D-lines usually are well-separated from spectral interference for low (~ 1 eV) temperature plasma containing sodium as long as reasonable resolving power is available. For example, for the sodium D-lines, a resolving power, R , of $R \simeq 1,000$ is needed to distinguish the two components D1 and D2, separated by ~ 0.06 nm. Resolving individual lines of molecular spectra may require $R > 10,000$, or at least of the order of one magnitude better resolution than needed for atoms, of course depending on temperature. In molecular spectroscopy, one tends to focus on molecular bands describing electronic transitions. Study of individual atomic or molecular resonances with continuous-wave radiation typically requires GHz scans with nominal MHz or better laser bandwidths. In this work, the focus is on optical spectrometers that measure near-uv to near-ir molecular bands with a spectral resolution, $\delta\lambda$ of the order of $\delta\lambda \sim 0.1$ nm.

Selected diatomic molecular spectra of AlO, C₂, CN, OH, N₂⁺, NO, and TiO, transitions are of interest as these can be observed in laser-induced breakdown spectroscopy (LIBS) [9– 11] at standard ambient temperature and pressure (SATP). Diatomic AlO and TiO spectra usually occur following creation of micro-plasma near or at aluminum and titanium surfaces, respectively. In several cases, molecular spectra may not be of primary interest in elemental analysis with LIBS using nanosecond laser pulses, but molecular spectra are readily observed with femtosecond laser-plasma excitation, or after some time delay (of the order of larger than 100 ns for occurrence of CN in CO₂:N₂ gas mixtures) from optical breakdown when using nanosecond laser pulses. Just like for atomic spectra, reasonably accurate molecular spectra are required for analysis [12–16]. The construction of a molecular spectrum relies on: (i) accurate line positions, and (ii) reasonably accurate transition strengths [17–20]. For the former, numerical singular value decomposition is employed for upper and lower levels of a particular transition. For the latter, Frank-Condon

factors and r-centroids are computed, and then combined with the rotational factors that usually decouple from the overall molecular line-strength due to the symmetry of diatomic molecules.

This work communicates data files and associated scripts for the computation of diatomic molecular spectra, and equally, for the fitting of measured data using a nonlinear fitting algorithm. Calculated spectra are presented and references to recorded data sets are provided. Applications comprise fields of chemistry, materials science, astronomy, and last but not least, physics including astrophysics, e.g., decoding of light from white dwarf stars such as Procyon B. The data are provided as a set of wave numbers, upper level term value, and line strength. Originally, FORTRAN/Windows 7 programs computed diatomic molecular spectra [17], but the scripts for the generation of molecular spectra are redesigned for use with MATLAB [21]. Moreover, this work communicates MATLAB-optimized line-strength files (LSFs) containing three columns, namely wave numbers, upper term values, and line strengths. Supplementary data contain programs and nine, selected diatomic molecular transitions of AlO, C₂ Swan, CN red, CN violet, OH uv, N₂⁺, NO gamma, TiOγ, and TiOγ'.

2. COMPUTATIONAL DETAILS

The computation of diatomic molecular spectra utilizes established line strength data. Programs in FORTRAN accomplish the generation of spectra, coupled with a separate plotting program for visualization, including convenient implementation using a Microsoft-Windows 7 operating system. This work communicates equivalent MATLAB scripts that appear popular with various research groups. First, the Boltzmann equilibrium spectral program (BESP) generates a theoretical spectrum, and second, the Nelder-Mead temperature (NMT) program accomplishes fitting of experimental and theoretical spectra. In principle, BESP can be used to generate maps as function of temperature and line-width with subsequent determination of the optimum solution with minimal errors in the least-square sense. In turn, NMT utilizes non-linear optimization by using geometric constructs, viz. simplexes. The accumulation of experimental spectra in this work is in accord with laser-induced breakdown spectroscopy, or in general, laser spectroscopy [22].

A. MATLAB scripts

The parameter list includes wavelength minimum, maximum, temperature, number of points, normalization factor, and file name. For the BESP.m and NMT.m scripts, the

Table I. Constants in BESP.m and NMT.m.

Constant	Value
Plank constant (h)	$6.62606957 \times 10^{-34}$ (J s)
speed of light (c)	2.99792458×10^8 (m s ⁻¹)
Boltzmann constat (kb)	$1.3806488 \times 10^{-23}$ (J K ⁻¹)

Table II. Parameters and variables in BESP.m and NMT.m.

Description	Variable
wavelength minimum	wl_min (cm ⁻¹)
wavelength maximum	wl_max (cm ⁻¹)
temperature	T (kK)
full-width at half maximum	FWHM, δλ (nm)
number of points	N
normalization	norm
file name	x

outputs are generated in graphical form. The scripts account for variation of the refractive index, r_i , of air with wavelength,

$$r_i = 1 + a_0 + \frac{a_1}{\lambda^2} + \frac{a_2}{\lambda^4}. \quad (1)$$

Table I shows script constants, and Table II summarizes input variables that are important for spectra computations. However, redesign of BESP.m and NMT.m from the FORTRAN/Windows 7 version [17] was accomplished with extensive discussions [20]. Edited versions of BESP.m and NMT.m are communicated in this work, however, the corresponding line strength data files will be posted separately.

1. BESP.m

The script BESP.m is designed following the FORTRAN/Windows 7 version [17]. The individual diatomic molecular data files for selected transitions are concatenated to only show wavenumbers, upper term value, and line strength, see Table IV. Adjustments of input parameters for MATLAB [21] are rather straightforward, equally, for generalizing the script for automatic input by converting the script to a function. Individual lines are computed using Gaussian profiles [17], and for the generation of a spectrum, only one temperature is needed for equilibrium computation. Conversely, as one infers temperature from a measured spectrum, a modified Boltzmann plot [18] is constructed for determination of the equilibrium temperature.

The program BESP.m receives input from the LSFs that contain relative line strengths. The output is generated in graphical standard format, and the program is slightly adjusted for generation of the spectra illustrated in Figures 1 to 9. However, Figure 6 is generated with the BESP.m script given below.

```
% BESP.m
%
% Calculates diatomic spectra using line strength data files constructed for selected transitions.
% The program is designed using a previous FORTRAN/Windows7 implementation including private communications
% with James O. Hornkohl and David M Surmick.
%
% David M. Surmick, 04-27-2016; edited by Christian G. Parigger 3-15-2022.

% input parameters, output: WL_exp (N-1 x 1 array), I (intensity)
wL_min=305; wL_max=325; T=3390; FWHM=0.35; N=1001; norm=1; x='OH-LSF.txt';

% generate wavelengths/wavelength-bins for computation akin to an experiment
nSpec=N-1; delWL=(wL_max-wL_min)/(nSpec); WL_exp=linspace(wL_min,wL_max,nSpec); WL_exp=WL_exp';

% constants in MKS units (Boltzmann factor bFac in cgs units)
h=6.62606957e-34; c=2.99792458e8; kb=1.3806488e-23; bFac=(100*h*c)/kb; gFac=2*sqrt(log(2));

% read line strength file
[p]=load(x); WN=p(:,1); Tu=p(:,2); S=p(:,3);

% convert vacuum wavenumber to air wavelength
a0=2.72643e-4; a1=1.2288; a2=3.555e4; r=1+a0+(a1./(WN.*WN))+(a2./(WN.*WN.*WN.*WN)); WL=1e7./(r.*WN);

% get LSF table wavelengths that most closely match the wavelength-bins
A=find(WL>wL_min & WL<wL_max);WLk=WL(A);

% get term values and line strengths at WLk in the range wL_min to wL_max
Sk=S(A); Tuk=Tu(A); TuMin=min(Tuk);

% calculate peak intensities and initialize peak_k calculation
peak=-4*log(WLk)+log(Sk)-(bFac/T)*(Tuk-TuMin); peak_k=zeros(nSpec,1); peakMax=-1;
for i=1:length(peak);
    if peak(i) > peakMax; peakMax=peak(i); end;
```

```

    if peak(i) ~= 0; peak_k(i)=peak(i)-peakMax; end;
end; peak_k=exp(peak_k);

% get wavelength-bin positions that most closely matches line strength table wavelengths
n0=zeros(length(WLk),1); for i=1:length(WLk); [~,n0(i)]=min(abs(WL_exp-WLk(i))); end;

% calculate spectrum using Gaussian profiles for peaks, and for wavelength dependent FWHM
I=zeros(nSpec,1); FWHMk=(FWHM*WLk)/wL_max;
for i=1:length(WLk); deln=round(FWHM/deLWL,0); nMin=n0(i)-deln;
    if nMin < 1; nMin=1; end; nMax=n0(i)+deln;
    if nMax > nSpec; nMax=nSpec; end;
    for j=nMin:nMax; u=abs(gFac*(WL_exp(j)-WLk(i))/FWHMk(i));
        if u <=9.21; I(j)=I(j)+peak_k(i)*exp(-u*u); end;
    end;
end; I=norm*I/max(I);

%Display graphical output
figure; plot(WL_exp,I,'LineWidth',1.5); set(gca,'FontWeight','bold','FontSize',20,'TickLength',[0.02, 0.02]);
LimitsX=xlim; LimitsY=ylim; title(' ', 'HorizontalAlignment','left','Position', [LimitsX(1)-4, LimitsY(2)]);
xlabel('wavelength (nm)','FontSize',24,'FontWeight','bold');
ylabel('intensity (a.u.)','FontSize',24,'FontWeight','bold');

```

2. NMT.m

The NMT script details are deferred to Appendix A. The adaptation of a previous FORTRAN code with Windows 7 libraries for a Microsoft platform is no longer viable due to support discontinuation of the Windows 7 operating system. However, the NMT.m script delivers spectra fitting results identical to those obtained with the FORTRAN/Windows 7 implementation.

3. Data files

This section summarizes the results obtained by using line strength data. The line strength files (LSFs) contain wave-numbers, upper term values, and the line strengths. Table III summarizes contents of line strength data. The two programs BESP and NMT convert the vacuum wave numbers to air wavelengths for analysis of measured data, see Equation 1. Table III associates the diatomic molecules and their line strength data, including the wavelength range.

The LSFs contain significantly more data than illustrated in this communication. Appli-

Table III. Line strength data contents: Wave numbers, upper term values, line strengths.

Description	Variable	Column
wave number	WN (cm ⁻¹)	1
upper term value	Tu (cm ⁻¹)	2
line strength	S (stC ² cm ²) ^a	3

^a 1 stC = 3.356 10⁻¹⁰ C.

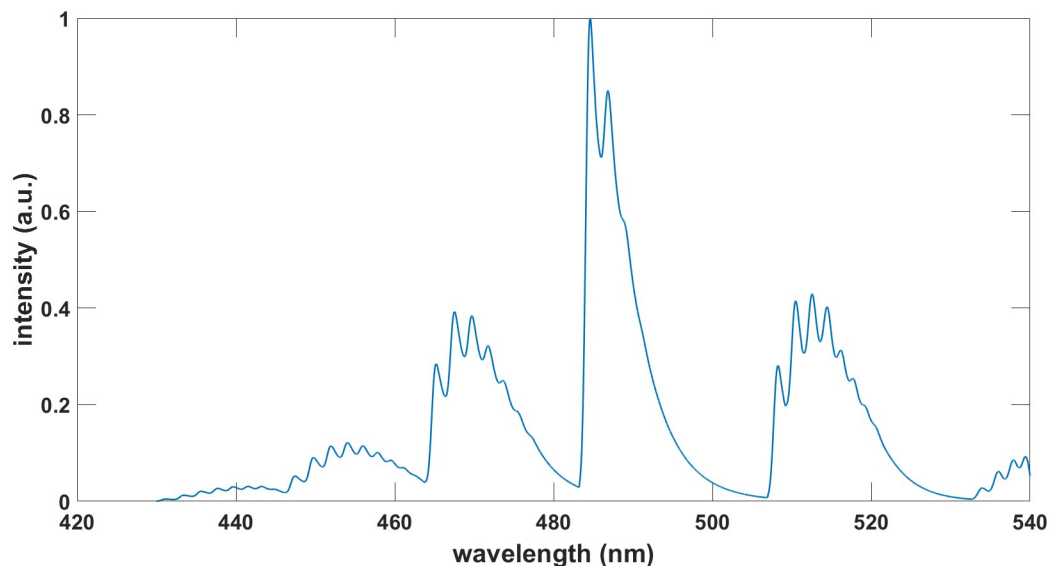
Table IV. Diatomic molecules, data file, wavelength range, and number of spectral lines.

Diatomic Molecule	Data File	Wavelength (nm)	Spectral Lines
aluminum monoxide (AlO)	AlO-BX-LSF.txt	430.72 – 997.66	33,484
carbon Swan spectra (C ₂)	C2-Swan-LSF.txt	410.93 – 678.58	29,004
cyaide red (CNr) system	CNr-LSF.txt	499.89 – 4997.56	40,728
cyaide violet (CNv) system	CNv-LSF.txt	372.88 – 425.22	7,960
hydroxyl (OH) violet system	OH-LSF.txt	278.65 – 379.72	1,683
nitrogen monoxide (NO) γ system	NO-GAMMA-LSF.txt	200.41 – 285.95	13,000
singly ionized nitrogen (N ₂ ⁺)	N2p-LSF.txt	319.04 – 501.46	7,302
titanium monoxide (TiO) γ band	TiO-AX-LSF.txt	599.58 – 945.44	66,962
titanium monoxide (TiO) γ' band	TiO-BX-LSF.txt	582.73 – 679.12	34,648

cations of the LSFs includes data analysis of laser-induced fluorescence and computation of absorption spectra. Some of these applications are elaborated in the discussion of C₂ Swan spectra [19].

III. RESULTS

This section summarizes the communicated line strength data. Table V associates the diatomic molecules and their line strength files (LSF). The LSFs contain wave numbers, upper term values and the line strength. The two programs BESP and NMT convert the vacuum wave numbers to air wavelengths for analysis of measured data. Table V displays spectral resolution, temperature, and Table V also communicates but one reference each for measurement and fitting selected molecular transitions of AlO, C₂, CN, OH, N₂⁺, NO, and TiO. Figures 1 to 9 illustrate computed spectra that refer to measured ones in the references.


FIG. 1. Computed AlO spectrum, $\Delta v = 0, \pm 1, \pm 2, +3$, $\delta\lambda = 1.0\text{nm}$, $T = 3.33\text{ kK}$.

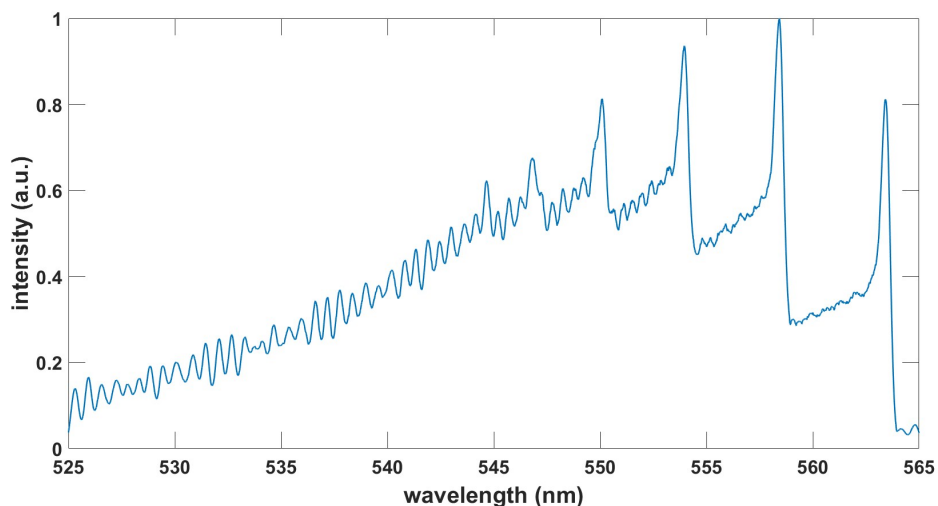


FIG. 2. Computed C_2 Swan spectrum, $\Delta v = -1$, $\delta\lambda = 0.39\text{nm}$, $T = 6.75\text{ kK}$.

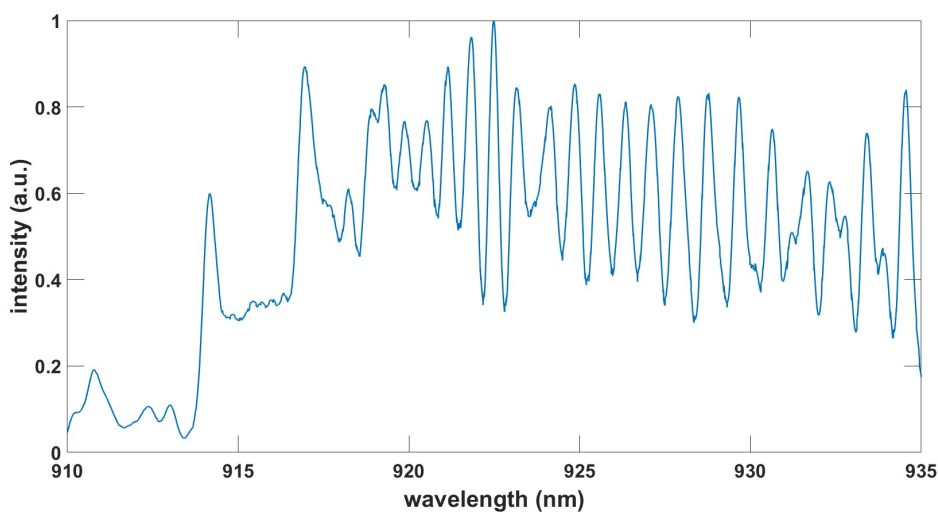


FIG. 3. Computed CN red spectrum, $\Delta v = +1$, $\delta\lambda = 0.38\text{nm}$, $T = 7.5\text{ kK}$.

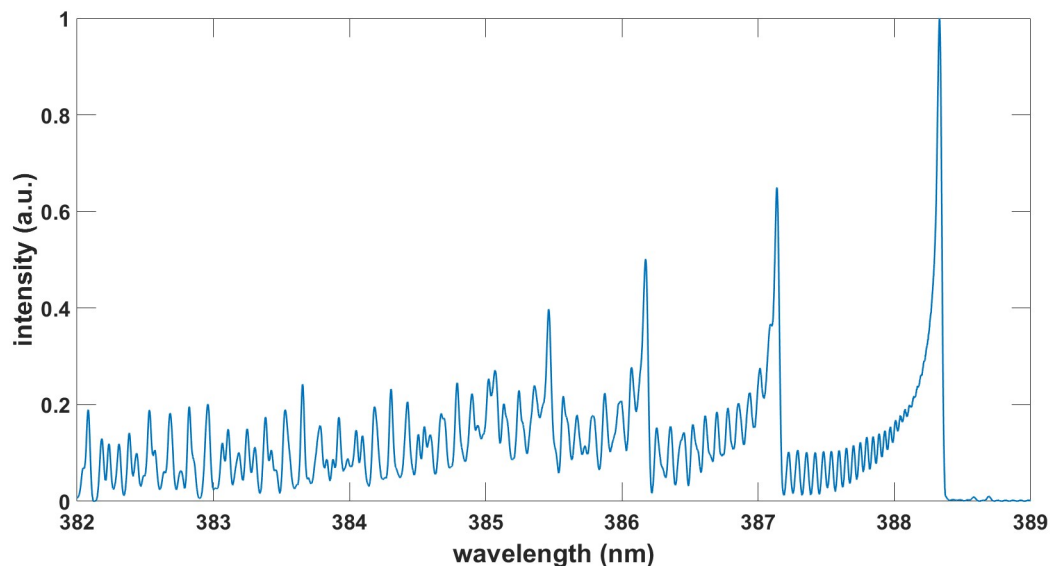


FIG. 4. Computed CN violet spectrum, $\Delta v = 0$, $\delta\lambda = 0.030\text{nm}$, $T = 7.94\text{ kK}$.

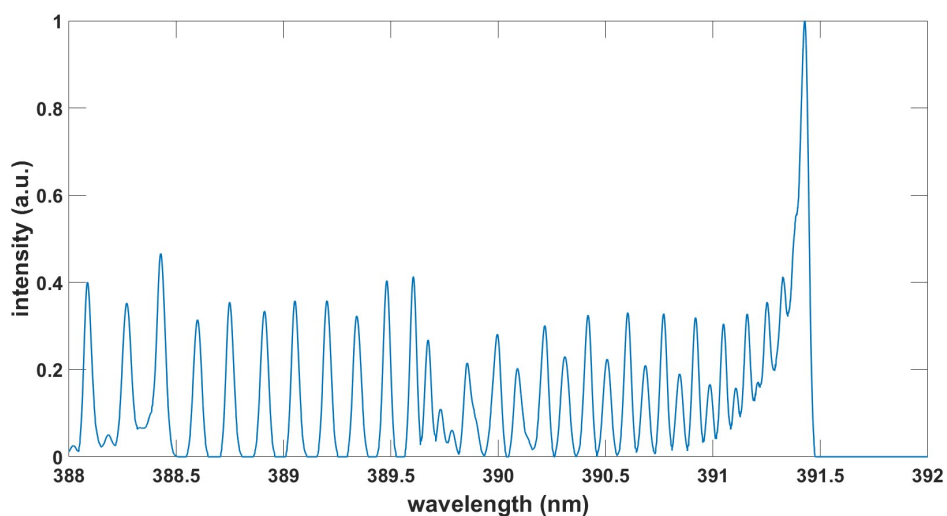


FIG. 5. Computed N₂⁺ spectrum, $\Delta v = 0$, $\delta\lambda = 0.035\text{nm}$, $T = 5.1\text{ kK}$.

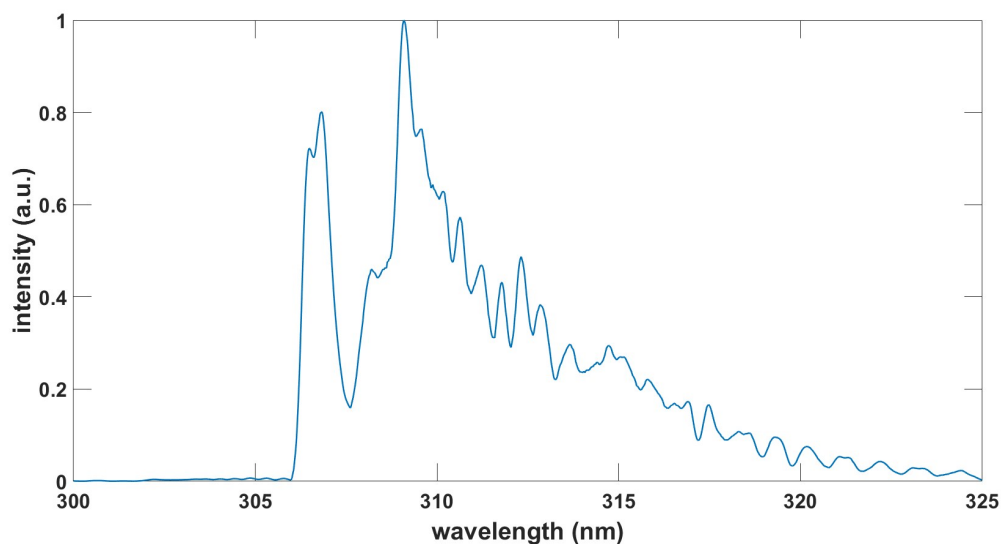


FIG. 6. Computed OH spectrum, $\Delta v = 0$, $\delta\lambda = 0.35\text{nm}$, $T = 3.39\text{ kK}$, see BESP.m script and Ref. [28].

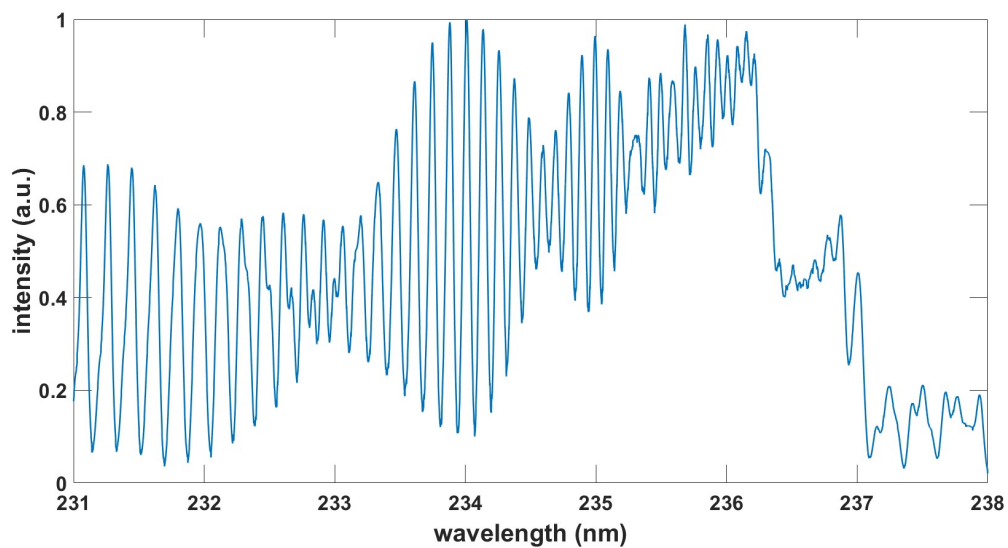


FIG. 7. Computed NO gamma spectrum, $\Delta v = -1$, $\delta\lambda = 0.056\text{nm}$, $T = 6.80\text{ kK}$.

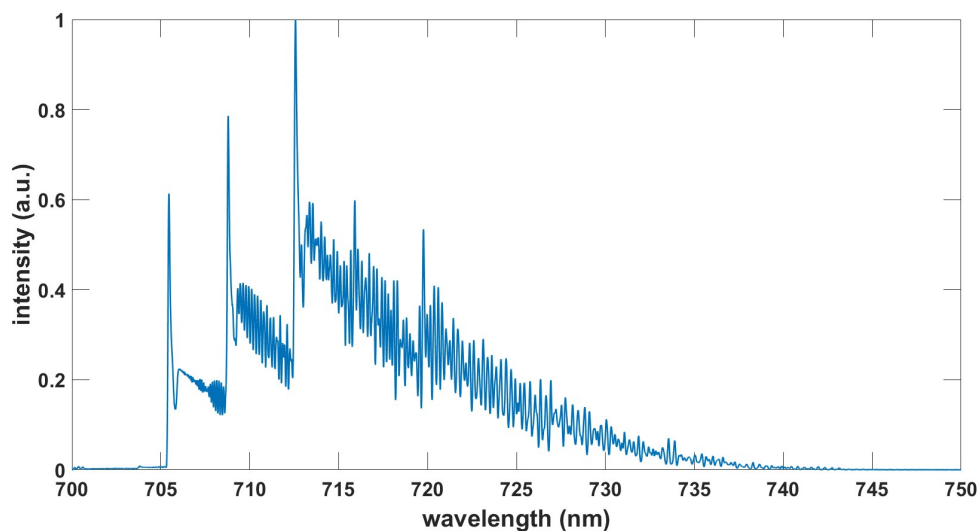


FIG. 8. Computed TiO γ spectrum, $\Delta v = 0$, $\delta\lambda = 0.10\text{nm}$, $T = 3.03\text{ kK}$.

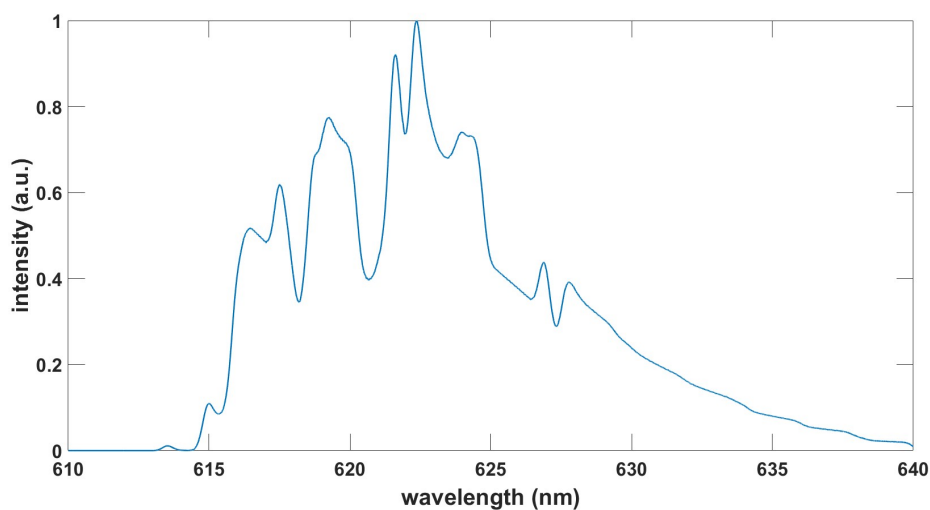


FIG. 9. Computed TiO γ' spectrum, $\Delta v = 0$, $\delta\lambda = 0.40\text{nm}$, $T = 3.6\text{ kK}$.

Table V. Diatomic molecules, spectral resolution, temperature, and one typical reference each that utilizes the data.

Diatomic Molecule	Data	Resolution (nm)	T (kK)	Ref.	Figure
aluminum monoxide (AlO)	AlO-BX-LSF.txt	1.0	3.33	[23]	1
carbon Swan spectra (C ₂)	C2-Swan-LSF.txt	0.39	6.75	[24]	2
cynaide red (CNr) system	CNr-LSF.txt	0.38	7.5	[25] ^a	3
cynaide violet (CNv) system	CNv-LSF.txt	0.030	7.94	[26]	4
singly ionized nitrogen (N ₂ ⁺)	N2p-LSF.txt	0.035	5.1	[27]	5
hydroxyl (OH) ultraviolet system	OH-LSF.txt	0.35	3.39	[28]	6
nitrogen monoxide (NO) γ system	NO-GAMMA-LSF.txt	0.056	6.8	[29]	7
titanium monoxide (TiO) γ band	TiO-AX-LSF.txt	0.10	3.03	[30] ^b	8
titanium monoxide (TiO) γ' band	TiO-BX-LSF.txt	0.40	3.6	[31]	9

^a Experiments at Johannes Kepler University, Linz, Austria

^b Experiments in part at Chemical Research Center of the Hungarian Academy of Science, Budapest, Hungary

IV. DISCUSSION

The accurate prediction of line positions of diatomic molecules is important for identification, and of course for fitting of measured data. The line positions are usually more accurate than the intensity values. The selected transitions for most of the communicated diatomic molecules, especially AIO, C₂ Swan, CN, and OH, have been extensively tested in the study of laser-induced optical breakdown. However, it will be of interest to compare predicted spectra with those from other databases.

ACKNOWLEDGMENTS

The author acknowledges the support in part by the Center for Laser Applications at the University of Tennessee Space Institute.

APPENDIX A

This Appendix communicates the NMT.m script for fitting of recorded experimental data, OH100microsec.dat. Figure 10 shows the output in graphical form.

```
% NMT.m
%
% Fits measured diatomic spectra using line strength data files constructed for selected transitions.
% The program is designed using a previous FORTRAN/Windows7 implementation including private communications
% with James O. Hornkohl and David M Surmick.
%
% inputs: WL_exp — experimental wavelengths (n x 1 array)
%         Dat   — experimental spectrum (n x 1 array)
%         FWHM  — measured spectral resolution, seed for varried FWHM or
%               fixed
%         T     — temperature seed for fitting
%         tol   — tolerance of Nelder-Mead fit
%         x     — name of line strength file for calculating theory spectra
%         FIT   — enter 1 for fitting linear offset and temperature
%               enter 2 for fitting linear offset, temperature, and FWHM
%
% outputs: profile — matrix containing experimental wavelengths, measured
%           spectrum, fitted spectrum, fitted baseline offset
%           (n x 4 matrix)
%         vals   — array containing fitted paramters (3x1 or 4x1 array),
%           temperature is always last entry
%
% sub-functions: FitSpec, FitSpec1, SynthSpec
%
% Example call: [I,v]=NMT(x,y1,0.15,3000,1e-8,'OH-LSF.txt',2);
%
% David M. Surmick, 04-28-2016, edited by Christian G Parigger 3-16-2022

function [profile,vals] = NMT (WL_exp,Dat,FWHM,T,tol,x,FIT)
tic % start code timer

% global variables
global bFac gFac WLk Tuk TuMin Sk n0 nSpec fwhm deLWL temp wL_max;

% constants in MKS units (Boltzmann factor bfac in cgs units)
h=6.62606957e-34; c=2.99792458e8; kb=1.3806488e-23; bFac=(100+h*c)/kb; gFac=2*sqrt(log(2));

%load experimental data, here an OH spectrum 100 microsecond time delay in air breakdown.
load OH100microsec.dat; Dat=OH100microsec(:,2); WL_exp=OH100microsec(:,1); nSpec=length(Dat);

% input paramters
```

```

T=2000; FWHM=0.3; x='OH-LSF.txt'; temp=T; fwhm=FWHM; wl_min=min(WL_exp); wl_max=max(WL_exp); delWL=(wl_max-wl_min)
/(nSpec);

% read MatLab LSF file
[p]=load(x); WN=p(:,1); Tu=p(:,2); S=p(:,3);

% convert vacuum wavenumber to air wavelength
a0=2.72643e-4; a1=1.2288; a2=3.555e4; r=1+a0+(a1./(WN.*WN))+(a2./(WN.*WN.*WN)); WL=1e7./(r.*WN);

% get LSF table wavelengths in experimental range
A=find(WL>wl_min & WL<wl_max); WLk=WL(A);

% get Term Values and LineStrengths at WLk
Sk=S(A); Tuk=Tu(A); TuMin=min(Tuk);

% get experimental wavelength positions that most closely matches line strength table wavelengths
n0=zeros(length(WLk),1); for i=1:length(WLk); [~,n0(i)]=min(abs(WL_exp-WLk(i))); end;

% normalize data
%Dat=Dat/max(Dat);

% Fitting with Nelder-Mead parameters including two cases options
tol=1.e-6; FIT=2; options=optimset('TolX',tol,'MaxIter',1e8,'MaxFunEvals',1e8);
switch FIT
    case 1 % fit offset, temperature
        theta=ones(3,1);
        theta(3)=T; % temperature seed
        vals=fminsearch(@(x) FitSpec(x,WL_exp,Dat),theta,options);
        bkg=vals(1)+vals(2)*WL_exp; % calculate fitted offset
        [I,bkg1]=SynthSpec(WL_exp,vals(3),FWHM,Dat,bkg); % calculate fit
    case 2 % fit offset, fwhm, temperature
        theta=ones(4,1);
        theta(3)=FWHM; % fwhm seed
        theta(4)=T; % temperature seed
        vals=fminsearch(@(x) FitSpec1(x,WL_exp,Dat),theta,options);
        bkg=vals(1)+vals(2)*WL_exp; % calculate fitted offset
        [I,bkg1]=SynthSpec(WL_exp,vals(4),vals(3),Dat,bkg); % calculate fit
end

% output profile array
%profile=[WL_exp Dat I bkg1];

% Visualize Fit
fname=regexprep(x,'-LSF.txt','-fit:');
figure
switch FIT

```

```

case 1
    plot(WL_exp,Dat,'o',WL_exp,I,WL_exp,bkg1,'—','LineWidth',1.75)
    legend('experiment','fit','base line')
    set(gca,'FontWeight','bold','FontSize',16,'TickLength',[0.02, 0.02]);
    val3=round(vals(3),3, 'significant')
    title([num2str(fname), 'T=',num2str(vals(3)), 'K ,FWHM=',num2str(FWHM), 'nm'])
    xlabel('wavelength (nm)')
    ylabel('intensity (a.u.)')
case 2
    plot(WL_exp,Dat,'o',WL_exp,I,WL_exp,bkg1,'—','LineWidth',1.75)
    legend('experiment','fit','base line')
    set(gca,'FontWeight','bold','FontSize',20,'TickLength',[0.02, 0.02]);
    round(vals(4),3,'significant'); round(vals(3),2,'significant');
    val4=round(vals(4),3, 'significant'); val3=round(vals(3),2, 'significant');
    title([num2str(fname), ' T=',num2str(val4), ' K, FWHM=',num2str(val3), ' nm'])
    xlabel('wavelength (nm)','FontSize',24,'FontWeight','bold')
    ylabel('intensity (a.u.)','FontSize',24,'FontWeight','bold')
end

toc % end code timer

end % main function

% temperature, offset fit function
function [err] = FitSpec (p,WL_exp,Dat);
global fwhm;
bkg=p(1)+p(2)*WL_exp; [F,~]=SynthSpec(WL_exp,p(3),fwhm,Dat,bkg); c=F\Dat; z=F*c; err=norm(z-Dat);
end % fit spec

% temperature, fwhm, offset fit function
function [err] = FitSpec1 (p,WL_exp,Dat);
bkg=p(1)+p(2)*WL_exp; [F,~]=SynthSpec(WL_exp,p(4),p(3),Dat,bkg); c=F\Dat; z=F*c; err=norm(z-Dat);
end % fit spec 1

% calculate synthetic spectrum for fit
function [I1,bkg1] = SynthSpec (WL_exp,T,FWHM,Dat,bkg);
global bFac gFac WLk Tuk TuMin Sk n0 nSpec delWL wL_max;
FWHMk=(FWHM*WLk)/wL_max; % wavelength dependent FWHM

% Calculate Peak Intensities
peak=-4*log(WLk)+log(Sk)-(bFac/T)*(Tuk-TuMin); peak_k=exp(peak);

% calculate synthetic spectrum
I=zeros(nSpec,1); % initialize synthetic spectrum output
for i=1:length(WLk); deln=round(2.5*FWHMk(i)/delWL); nMin=n0(i)-deln;
    if nMin < 1; nMin=1; end;

```

```

nMax=n0(i)+deIn;
if nMax > nSpec; nMax=nSpec; end;
for j=nMin:nMax; u=abs(gFac*(WLk(i)-WL_exp(j))/FWHMk(i)); I(j)=I(j)+peak_k(i)*exp(-u*u); end;
end % synthetic spectrum loop

% normalize data to measured spectrum
I=I/max(I); I=I+bkg; sxy=sum(Dat.*I); syy=sum(I.*I); nf= sxy/syy; I1=I*nf; bkg1=bkg*nf;
end % SynthSpec

```

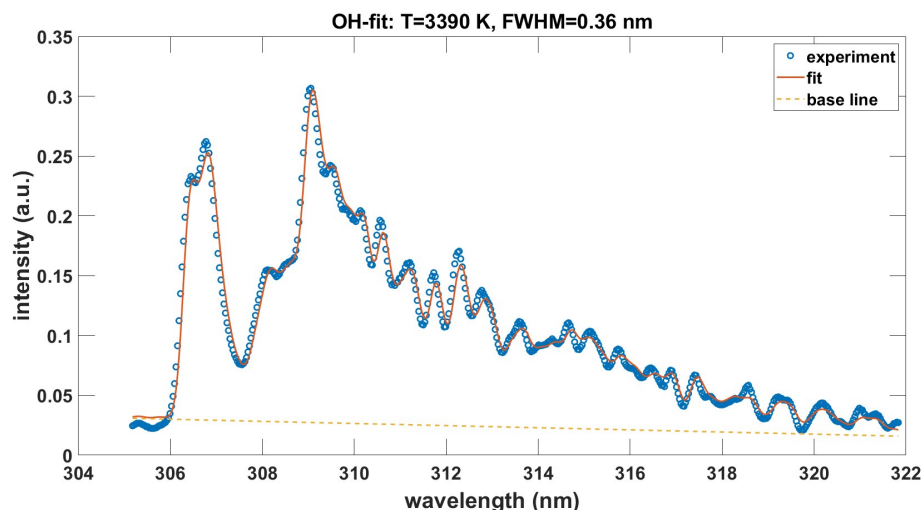


FIG. 10. Computed and fitted OH spectra, $\Delta v = 0$, $\delta\lambda = 0.36\text{nm}$, $T = 3.39\text{ kK}$, see Ref.[28]

References

- [1] Kunze, H.-J. Introduction to Plasma Spectroscopy; Springer: Berlin/Heidelberg, Germany, 2009.
- [2] Fujimoto, T. Plasma Spectroscopy; Clarendon Press; Oxford, UK, 2004.
- [3] Ochkin, V.N. Spectroscopy of Low Temperature Plasma; Wiley-VCH: Weinheim, Germany, 2009.
- [4] Omenetto N. (Ed.) Analytical Laser Spectroscopy; John Wiley & Sons: New York, NY, USA, 1979.
- [5] Demtröder, W. Laser Spectroscopy 1: Basic Principles, 5th ed.; Springer: Heidelberg, Germany, 2014.
- [6] Demtröder, W. Laser Spectroscopy 2: Experimental Techniques, 5th ed.; Springer: Heidelberg, Germany, 2015.
- [7] Hertel, I.V.; Schulz C.-P. Atoms, Molecules and Optical Physics 1, Atoms and Spectroscopy; Springer: Heidelberg, Germany, 2015.
- [8] Hertel, I.V.; Schulz C.-P. Atoms, Molecules and Optical Physics 2, Molecules and Photons - Spectroscopy and Collisions; Springer: Heidelberg, Germany, 2015.
- [9] Miziolek, A.W., Palleschi, V., Schechter, I. (Eds.) Laser Induced Breakdown Spectroscopy (LIBS): Fundamentals and Applications; Cambridge Univ. Press: New York, NY, USA, 2006.
- [10] Singh, J.P.; Thakur, S.N. (Eds.) Laser-Induced Breakdown Spectroscopy, 2nd ed.; Elsevier: Amsterdam, The Netherlands, 2020.
- [11] De Giacomo, A.; Hermann, J. J. Phys. D Appl. Phys. 50, 2017, 183002.
- [12] Parigger, C.G. Laser-induced breakdown in gases: Experiments and simulation. In Laser Induced Breakdown Spectroscopy (LIBS): Fundamentals and Applications; Miziolek, A.W., Palleschi, V., Schechter, I., Eds.; Cambridge Univ. Press: New York, NY, USA, 2006; Chapter 4, pp. 171–193.
- [13] Parigger, C.G.; Surmick, D.M.; Helstern, C.M.; Gautam, G.; Bol'shakov, A.A.; Russo, R. Molecular Laser-Induced Breakdown Spectroscopy, In Laser Induced Breakdown Spectroscopy, 2nd ed.; Singh, J.P., Thakur, S.N., Eds.; Elsevier: Amsterdam, The Netherlands, 2020; Chapter 7, pp. 167–212.
- [14] Parigger, C.G.; Helstern, C.M.; Jordan, B.S.; Surmick, D.M.; Splinter, R. Molecules 25, 2020, 615.
- [15] Parigger, C.G.; Helstern, C.M.; Jordan, B.S.; Surmick, D.M.; Splinter, R. Molecules 25, 2020, 988.
- [16] Parigger, C.G. Spectrochim. Acta Part B At. Spectrosc. 179, 2021, 106122.

- [17] Parigger, C.G.; Woods, A.C.; Surmick, D.M.; Gautam, G.; Witte, M.J.; Hornkohl, J.O. *Spectrochim. Acta Part B: At. Spectrosc.* 107, 2015, 132.
- [18] Parigger, C.G.; Hornkohl, J.O. *Quantum Mechanics of the Diatomic Molecule with Applications*; IOP Publishing: Bristol, UK, 2020.
- [19] Hornkohl, J.O.; Nemes, L.; Parigger, C.G.; *Spectroscopy of Carbon Containing Diatomic Molecules*. In *Spectroscopy, Dynamics and Molecular Theory of Carbon Plasmas and Vapors: Advances in the Understanding of the Most Complex High-Temperature Elemental System*; Nemes, L, Irle, S., Eds.; World Scientific: Singapore, SG, 2011; Chap. 4, pp. 113–165.
- [20] Surmick, D.M.; Hornkohl, J.O. (The University of Tennessee, University of Tennessee Space Institute, Tullahoma, Tennessee, US). Personal communication, 2016.
- [21] MATLAB Release R2022a Update 5, The MathWorks, Inc., Natick, Massachusetts, US, 12 August 2022.
- [22] Parigger, C.G.; Woods, A.C.; Witte, M.J.; Swafford, L.D.; Surmick, D.M. *J. Vis. Exp.* 84, 2014, e51250.
- [23] Dors, I.G., Parigger, C.; Lewis, J.W.L. *Opt. Lett.* 23, 1998, 1778.
- [24] Parigger, C.; Plemmons, D.H.; Hornkohl, J.O.; Lewis, J.W.L. *J. Quant. Spectrosc. Radiat. Transfer* 52, 1994, 707.
- [25] Trautner, S.; Jasik, J.; Parigger, C.G.; Pedarnig, J.D; Spindelhofer, W.; Lackner, J.; Veis, P.; Heitz, J. *Spectrochim. Acta Part A: Mol. Biomol. Spectrosc.* 174, 2017, 331.
- [26] Hornkohl, J.O.; Parigger, C.; Lewis J.W.L. *J. Quant. Spectrosc. Radiat. Transfer* 46, 1991, 405.
- [27] Parigger, C.; Plemmons, D.H.; Hornkohl, J.O.; Lewis, J.W.L. *Appl. Opt.* 34, 1995, 3331.
- [28] Parigger, C.G. *Hydroxyl Spectroscopy of Laboratory Air Laser-Ignition*. To be submitted to MDPI/Foundations, 2022.
- [29] Hornkohl, J.O.; Fleischmann, J.P.; Surmick, D.M.; Witte, M.J.; Swaffor, L.D.; Woods, A.C.; Parigger, C.G. *J. Phys.: Conf. Ser.* 548, 2014, 12040.
- [30] Parigger, C.G.; Woods, A.C.; Keszler, A.; Nemes, L.; Hornkohl, J.O. *AIP Conf. Proceedings* 1464, 2012, 628.
- [31] Woods, A.C.; Parigger, C.G.; Hornkohl, J.O. *Opt. Lett.* 37, 2012, 5139.



This document was created with the Win2PDF “print to PDF” printer available at <http://www.win2pdf.com>

This version of Win2PDF 10 is for evaluation and non-commercial use only.

This page will not be added after purchasing Win2PDF.

<http://www.win2pdf.com/purchase/>